Eur. Phys. J. C 34, 477–486 (2004)
Digital Object Identifier (DOI) 10.1140/epjc/s2004-01710-0

THE EUROPEAN PHYSICAL JOURNAL C

Triple gauge vertices at one-loop level in two-Higgs-doublet model

M. Malinský[1,2,a], J. Hořejší[1]

[1] IPNP, Faculty of Mathematics and Physics, Charles University, Prague, Czech Republic
[2] S.I.S.S.A., Trieste, Italy

Received: 30 September 2003 / Revised version: 2 February 2004 /
Published online: 31 March 2004 –

Abstract. Renormalized triple gauge vertices (TGV) are examined within the two-Higgs-doublet model of the electroweak interactions. Deviations of the TGV from their standard-model values are calculated at the one-loop level, in the on-shell renormalization scheme. As a consistency check, UV divergence cancellations anticipated on symmetry grounds are verified explicitly. The dependence of the TGV finite parts on the masses of possible heavy Higgs scalars is discussed briefly.

1 Introduction

The two-Higgs-doublet model (THDM) has been on stage in particle physics since the early days of spontaneously broken gauge theories (to the best of our knowledge, it has emerged first in [1], in connection with the problem of T-violation). THDM represents one of the simplest and most natural extensions of the electroweak standard model (SM): its Higgs sector contains an extra complex scalar doublet, in addition to the usual SM one. This means, among other things, that there are five physical scalar particles in the THDM spectrum, instead of the single SM Higgs boson. On the other hand, the doublet structure of the Higgs sector automatically guarantees the validity of the tree-level relation $\rho = 1$ for the familiar electroweak parameter $\rho = m_W^2/(m_Z^2 \cos^2\theta_{\rm W})$, in complete analogy with the SM.

Despite its conceptual simplicity, THDM can incorporate various kinds of "new physics" beyond SM and thus it has always been of considerable phenomenological interest; a concise overview of its possible applications can be found e.g. in [2]. It remains quite popular at the present time, as the Higgs physics (or, more generally, the physics of electroweak symmetry breaking) represents the central issue of the high-energy experiments planned for the nearest future. Note that a part of the current popularity of the THDM is due to the fact that its Higgs sector essentially coincides with that of the minimal supersymmetric SM (MSSM), but is obviously less constrained. For some recent work on the THDM phenomenology, see e.g. [3–6] and references therein; a recent review of the subject can be found in [7].

One of the interesting technical aspects of the general THDM is that it admits "non-decoupling effects" in the Higgs sector: the heavy Higgs scalars (i.e. $m_{\rm Higgs} \gg m_W$) cannot be simply integrated out in the low-energy domain ($s \sim m_W^2$) and may give non-negligible contributions to some scattering amplitudes. Note that this is not the case in the MSSM, where the heavy Higgs bosons decouple in accordance with the Appelquist–Carazzone theorem [8] (for the corresponding MSSM analysis see [9]). The non-decoupling effects in THDM have been studied previously for the process $e^+e^- \to W^+W^-$ [10] within an approximation corresponding to the equivalence theorem (ET) [11] for longitudinal vector bosons. Here and in a forthcoming paper [12] we pursue this theme further by performing more detailed calculations that enable one to go beyond the framework of the ET approximation. In the present paper we calculate, at the one-loop level, the THDM contributions to the triple gauge vertices (TGV). These vertex corrections play the most important role in the possible non-decoupling effects; some applications of the results presented here will be discussed in detail in [12]. Some preliminary results in this direction have already appeared in [13].

This paper is organized as follows. In Sect. 2 a brief review of the THDM structure is given. Section 3 is devoted to kinematics, notation and some other technical prerequisites. In Sect. 4 we specify the quantities of our main interest and sketch the method of their calculation. We display all relevant Feynman diagrams together with the corresponding analytic expressions. The proper cancellation of UV-divergences is demonstrated in Sect. 4.6. In Sect. 5 we present a brief discussion of the results, in particular the mass dependence of the finite parts of renormalized TGV. Most of the technical details (structure of the Higgs–vector-boson interactions, coupling constants, useful integrals) are deferred to appendices.

2 Basic structure of THDM

In this paper we adopt the "classic" notation of [14]. We do not restrict ourselves to any particular realization of the

[a] e-mail: malinsky@ipnp.troja.mff.cuni.cz

THDM Higgs potential unless stated otherwise. As we shall see, although the relevant one-loop on-shell counterterms can in principle involve contributions descending from the Higgs self-couplings dictated by the particular realization of the model, they cancel out in the counterterm prescription.

2.1 The Higgs potential and spectrum

The most general THDM Higgs potential can be written as

$$\begin{aligned} V(\Phi_1,\Phi_2) &= m_{11}^2\Phi_1^\dagger\Phi_1 + m_{22}^2\Phi_2^\dagger\Phi_2 - (m_{12}^2\Phi_1^\dagger\Phi_2 + \text{h.c.}) \\ &+ \frac{\lambda_1}{2}(\Phi_1^\dagger\Phi_1)^2 + \frac{\lambda_2}{2}(\Phi_2^\dagger\Phi_2)^2 \\ &+ \lambda_3(\Phi_1^\dagger\Phi_1)(\Phi_2^\dagger\Phi_2) + \lambda_4(\Phi_1^\dagger\Phi_2)(\Phi_2^\dagger\Phi_1) \\ &+ \left\{\frac{\lambda_5}{2}(\Phi_1^\dagger\Phi_2)^2 + \Big[\lambda_6(\Phi_1^\dagger\Phi_1) + \lambda_7(\Phi_2^\dagger\Phi_2)\Big](\Phi_1^\dagger\Phi_2) + \text{h.c.}\right\}. \end{aligned}$$

It is convenient to parametrize the doublets by means of eight real scalar fields:

$$\Phi_1 = \frac{1}{\sqrt{2}}\begin{pmatrix}\phi_1 + \mathrm{i}\phi_2\\ \phi_3 + \mathrm{i}\phi_4\end{pmatrix}, \qquad \Phi_2 = \frac{1}{\sqrt{2}}\begin{pmatrix}\phi_5 + \mathrm{i}\phi_6\\ \phi_7 + \mathrm{i}\phi_8\end{pmatrix}.$$

The asymmetric vacuum is chosen so that

$$\langle\phi_1\rangle = v_1, \qquad \langle\phi_7\rangle = v_2, \qquad \langle\phi_i\rangle = 0 \quad \text{for} \quad i \neq 1,7,$$

where v_1 and v_2 are real constants. It is useful to introduce the angle β through $\tan\beta \equiv v_2/v_1$.

The mass-squared matrix $M_{ij}^2 \equiv \langle \partial^2 V/\partial\phi_i\partial\phi_j\rangle$ turns out to be block-diagonal, with each block having dimension 2. The diagonalization is straightforward and gives rise to the spectrum consisting of
(1) two charged states $H^\pm$ and $G^\pm$ with masses $m_{H^\pm}^2 \neq 0$ and $m_{G^\pm}^2 = 0$:

$$\begin{aligned} G^- &= \frac{1}{\sqrt{2}}\left[(\phi_1 + \mathrm{i}\phi_2)\cos\beta + (\phi_5 + \mathrm{i}\phi_6)\sin\beta\right] \\ H^- &= \frac{1}{\sqrt{2}}\left[-(\phi_1 + \mathrm{i}\phi_2)\sin\beta + (\phi_5 + \mathrm{i}\phi_6)\cos\beta\right]; \end{aligned}$$

(2) two neutral pseudoscalar states A^0 and G^0 with $m_{A^0}^2 \neq 0$ and $m_{G^0}^2 = 0$, which are mixed through the same angle β:

$$\begin{aligned} G^0 &= \phi_4\cos\beta + \phi_8\sin\beta, \\ A^0 &= -\phi_4\sin\beta + \phi_8\cos\beta; \end{aligned}$$

(3) two neutral scalar states H^0 and h^0 with $m_{H^0}^2 > m_{h^0}^2 \neq 0$, mixed through another angle, α:

$$\begin{aligned} H^0 &= (\phi_1 - v_1)\cos\alpha + (\phi_7 - v_2)\sin\alpha, \\ h^0 &= -(\phi_1 - v_1)\sin\alpha + (\phi_7 - v_2)\cos\alpha. \end{aligned}$$

Then the doublets Φ_1 and Φ_2 can be written in terms of the physical fields as follows:

$$\Phi_1 = \frac{1}{\sqrt{2}}\begin{bmatrix}\sqrt{2}G^+\cos\beta - \sqrt{2}H^+\sin\beta \\ H^0\cos\alpha - h^0\sin\alpha + v_1 + \mathrm{i}G^0\cos\beta - \mathrm{i}A^0\sin\beta\end{bmatrix},$$

$$\Phi_2 = \frac{1}{\sqrt{2}}\begin{bmatrix}\sqrt{2}G^+\sin\beta + \sqrt{2}H^+\cos\beta \\ H^0\sin\alpha + h^0\cos\alpha + v_2 + \mathrm{i}G^0\sin\beta + \mathrm{i}A^0\cos\beta\end{bmatrix}. \tag{1}$$

Note that the $G^\pm$ and G^0 are the unphysical Goldstone bosons to be eaten in the Higgs mechanism and h^0, H^0, A^0 and $H^\pm$ represent the physical scalars.

2.2 Interactions of THDM Higgs bosons with vector bosons

Interactions of the Higgs bosons with intermediate vector bosons descend from the gauge-invariant kinetic term

$$\mathcal{L}_{\text{Higgs}}^{\text{kin}} = (D_\mu\Phi_1)^\dagger(D^\mu\Phi_1) + (D_\mu\Phi_2)^\dagger(D^\mu\Phi_2). \tag{2}$$

Here the covariant derivative is defined by

$$\begin{aligned} D_\mu \equiv \partial_\mu &+ \mathrm{i}\frac{g}{\sqrt{2}}(W_\mu^+T^+ + W_\mu^-T^-) + \mathrm{i}eA_\mu Q \\ &+ \mathrm{i}\frac{g}{\cos\theta_{\text{W}}}Z_\mu(T_3 - Q\sin^2\theta_{\text{W}}), \end{aligned}$$

where the weak isospin operators $T^\pm \equiv T_1 \pm \mathrm{i}T_2$ and T_3 are expressed in terms of the Pauli matrices as $T_i \equiv \frac{1}{2}\tau_i$ and the charge operator is given by $Q = T_3 + Y_W$, with Y_W denoting the weak hypercharge. Inserting now the expansion (1) into (2) one gets the relevant part of the physical lagrangian; its detailed form is deferred to Appendix A.

2.3 Interactions with fermions

In general there are several different realizations of THDM [3, 14]. They differ mainly in the structure of the Yukawa couplings of the THDM Higgs bosons to fermions. As we shall see, the one-particle irreducible (1PI) one-loop graphs relevant for our purpose (i.e. those representing the leading-order corrections to the tree-level structure of TGV in THDM) do not include such Yukawa vertices. Therefore, we need not distinguish various THDM types in the subsequent computation.

3 Structure of triple gauge vertices

As in the SM case, there are two triple gauge vertices in THDM: γWW and ZWW. Let us denote the corresponding 1PI Green functions by

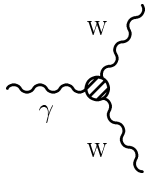

$$\equiv -\mathrm{i}c_\gamma\Gamma_{\sigma\mu\nu}^{\gamma WW}(q_i),$$

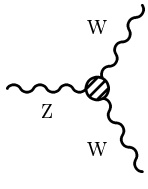

$$\equiv -\mathrm{i}c_Z\Gamma_{\sigma\mu\nu}^{ZWW}(q_i). \tag{3}$$

Here $c_\gamma \equiv e$, $c_Z \equiv e/\tan\theta_{\rm W}$ are tree-level triple gauge couplings, and q_1, q_2 and q_3 denote the four-momenta of the W^+, W^- and γ (or Z), all of them taken as *outgoing*.

3.1 Tree-level triple gauge vertices

Taking into account the momentum conservation, the *tree-level TGV* has the familiar form (see e.g. [15])

$$\begin{aligned}&\Gamma^{VWW}_{\sigma\mu\nu}(q_1,q_2) = \\ &(q_1-q_2)_\sigma g_{\mu\nu} + (2q_2+q_1)_\mu g_{\sigma\nu} - (2q_1+q_2)_\nu g_{\sigma\mu},\end{aligned} \tag{4}$$

where V stands for γ or Z. It is convenient to define

$$C^1_{\sigma\mu\nu} \equiv q_{1\sigma} g_{\mu\nu}, \qquad C^2_{\sigma\mu\nu} \equiv 2q_{2\mu} g_{\sigma\nu}, \qquad C^3_{\sigma\mu\nu} \equiv q_{1\mu} g_{\sigma\nu}. \tag{5}$$

In terms of these quantities we can write

$$\Gamma^{VWW}_{\sigma\mu\nu} = C^1_{\sigma\mu\nu} + C^3_{\sigma\mu\nu} + C^3_{\sigma\mu\nu} + \text{sym.} \equiv T_{\sigma\mu\nu}, \tag{6}$$

where "+sym." denotes the interchange $q_1 \leftrightarrow -q_2$, $\mu \leftrightarrow \nu$ in the preceding expression.

3.2 Triple gauge vertices at one-loop order

The full one-loop renormalized TGV receive a much more involved structure. Let us divide the set of all relevant one-loop diagrams into two subsets, where $\Gamma = \Gamma_F + \Gamma_B$ represent the graphs involving one fermionic and one bosonic loop respectively. As we have already noted, the fermionic one-loop contributions to TGV in SM and THDM are the same and therefore there is no need to discuss them.

It is clear that the on-shell TGV can only involve tensors at most trilinear in the external momenta (with bilinear terms obviously absent). Thus, we can decompose the bosonic part into a basis consisting of the linear terms (5) and trilinear ones:

$$\begin{aligned}C^4_{\sigma\mu\nu} &\equiv \frac{1}{m_W^2} q_{1\sigma} q_{1\mu} q_{1\nu}, \qquad C^5_{\sigma\mu\nu} \equiv \frac{1}{m_W^2} q_{1\sigma} q_{1\mu} q_{2\nu}, \\ C^6_{\sigma\mu\nu} &\equiv \frac{1}{m_W^2} q_{1\sigma} q_{2\mu} q_{1\nu}, \qquad C^7_{\sigma\mu\nu} \equiv \frac{1}{m_W^2} q_{2\sigma} q_{1\mu} q_{1\nu},\end{aligned} \tag{7}$$

and write Γ in the form

$$\Gamma^{VWW}_{\sigma\mu\nu} = \Big(T_{\sigma\mu\nu} + \sum \Gamma^{VWW}_{\sigma\mu\nu} + \delta Z_{\rm TGV} T_{\sigma\mu\nu}\Big) + \Gamma^{VWW}_F. \tag{8}$$

The first term in the brackets is the tree-level part (6), the second one comes from the sum of all relevant bosonic one-loop 1PI graphs and the third one represents the corresponding counterterm. The second term can now be expanded as

$$\sum \Gamma^{VWW}_{\sigma\mu\nu} = \sum_{i=1}^{7} \Pi_i^{VWW}(q_1^2, q_2^2, m_j^2) C^i_{\sigma\mu\nu} + \text{sym.}, \tag{9}$$

and using this we can rewrite the full one-loop renormalized Green function (8) in the form

$$\begin{aligned}\Gamma^{VWW}_{\sigma\mu\nu} &= \sum_{i=1}^{3} \left(1 + \delta Z_{\rm TGV} + \Pi_i^{VWW}\right) C^i_{\sigma\mu\nu} \\ &+ \sum_{i=4}^{7} \Pi_i^{VWW} C^i_{\sigma\mu\nu} + \Gamma_F^{VWW} + \text{sym.}\end{aligned} \tag{10}$$

Concerning the notation, let us add that the symbol δZ corresponds to the usual split of the renormalization constant $Z = 1 + \delta\, Z$.

4 Deviations of THDM one-loop triple gauge vertices from SM

As in the SM case [16] the full one-loop corrected TGV in THDM are very complicated because of the rich field contents of the theory. Since the models differ only in the Higgs sector, we can utilize the previous results in the non-Higgs sector and compute only the graphs which are not common to both models. These additional pieces can even be used separately in many situations. For example, it is shown in [12] that the leading one-loop correction to the SM value of the differential cross sections of $e^+e^- \to W^+W^-$ in THDM can be written in the form

$$\frac{{\rm d}\sigma^{\rm THDM}}{{\rm d}\sigma^{\rm SM}} = 1 + 2{\rm Re}\frac{\Delta\mathcal{M}_{1-\rm loop}\left[\Delta\Gamma^{VWW}\right]}{M^{\rm SM}_{\rm tree}} + \ldots$$

Here the structure of the term $\Delta\mathcal{M}_{1-\rm loop}$ is determined by the *differences of the one-loop renormalized Green functions in THDM and SM* defined by

$$\Delta\Gamma^{VWW}_{\sigma\mu\nu} \equiv \left[\Gamma^{VWW}_{\sigma\mu\nu}\right]_{\rm THDM} - \left[\Gamma^{VWW}_{\sigma\mu\nu}\right]_{\rm SM}. \tag{11}$$

Using (10) we can recast the last expression as

$$\begin{aligned}\Delta\Gamma^{VWW}_{\sigma\mu\nu} &= \sum_{i=1}^{3} \left(\Delta\delta Z_{\rm TGV} + \Delta\Pi_i^{VWW}\right) C^i_{\sigma\mu\nu} \\ &+ \sum_{i=4}^{7} \Delta\Pi_i^{VWW} C^i_{\sigma\mu\nu} + \text{sym.}\end{aligned} \tag{12}$$

(note the cancellation of the fermionic part). Here we have denoted

$$\begin{aligned}\Delta\delta Z_{\rm TGV} &\equiv (\delta Z_{\rm TGV})_{\rm THDM} - (\delta Z_{\rm TGV})_{\rm SM}, \\ \Delta\Pi_i^{VWW} &\equiv (\Pi_i^{VWW})_{\rm THDM} - (\Pi_i^{VWW})_{\rm SM}.\end{aligned} \tag{13}$$

Our goal is therefore to write down the quantities $\Delta\delta Z_{\rm TGV}$ and $\Delta\Pi_i^{VWW}$ for $i = 1, \ldots, 7$. Note that there is a non-trivial consistency check for the resulting expressions: The divergent parts of the $\Delta\Pi_i^{VWW}$ for $i = 1, 2, 3$ and $V = \gamma, Z$ must be equal in order to be successfully "eaten" by the divergences of $\Delta\delta Z_{\rm TGV}$. Moreover, the quantities $\Delta\Pi_i^{VWW}$ for $i = 4, \ldots, 7$ have to be finite because the gauge-invariant lagrangian does not contain corresponding counterterms.

4.1 Renormalization framework

In this paper we use the set of renormalization constants introduced in [15] (except that we use the symbol $\delta Z_{\rm TGV}$ instead of δZ_g of [15] to express the fact that $\delta Z_{\rm TGV}$ is *not* the usual counterterm corresponding to the fermion–gauge-boson vertex). The parameters are fixed so that the renormalized propagators have poles at the corresponding physical masses and the residues are normalized to 1. As we show below, a Ward identity connects the TGV counterterm $\delta Z_{\rm TGV}$ to the wave-function renormalization constant δZ_W of the W boson propagator.

The only information we need is the structure of the vector-boson propagator counterterms in the on-shell renormalization scheme. The one-loop renormalized inverse propagator has the general form

$$\begin{aligned}\Gamma^{VV}_{\mu\nu}(k) = \Gamma^{(0)}_{\mu\nu}(k) + \Pi_{\mu\nu}(k) + \delta Z_V k^2 P^{\rm T}_{\mu\nu} - \delta m_V^2 g_{\mu\nu} \\ + \text{gauge dependent term},\end{aligned}$$

where $\Gamma^{(0)}_{\mu\nu}(k)$ is the zeroth-order inverse propagator (in Feynman gauge $\Gamma^{(0)}_{\mu\nu}(k) = (k^2 - m^2)(P^{\rm T}_{\mu\nu} + P^{\rm L}_{\mu\nu})$). The on-shell counterterms are fixed by

$$\delta Z_V = -\left[\Pi^{\rm T}_{VV}(m_V^2) + m_V^2 \left.\frac{\rm d}{{\rm d}q^2}\right|_{q^2=m_V^2} \Pi^{\rm T}_{VV}(q^2)\right], \quad (14)$$

$$\delta m_V^2 = -m_V^4 \left.\frac{\rm d}{{\rm d}q^2}\right|_{q^2=m_V^2} \Pi^{\rm T}_{VV}(q^2), \quad (15)$$

and $\Pi^{\rm T}_{VV}(q^2)$ is the coefficient of the transverse projection operator in the decomposition of the vector-boson self-energy ${\rm i}\Pi^{VV}_{\mu\nu}(k)$, namely

$${\rm i}\Pi^{VV}_{\mu\nu}(k) \equiv {\rm i}k^2 \Pi^{\rm T}_{VV}(k^2) P^{\rm T}_{\mu\nu} + {\rm i}k^2 \Pi^{\rm L}_{VV}(k^2) P^{\rm L}_{\mu\nu}.$$

4.2 Relation $\Delta\delta Z_{\rm TGV} = \Delta\delta Z_W$

The photon mass counterterm is in our scheme expressed as

$$\delta m_\gamma^2 = -\,{\rm s}_\theta^2\,{\rm c}_\theta^2 m_Z^2 Z_H \left(1 - \frac{\delta v}{v}\right)^2 (1 - Z_W Z_{\rm TGV}^{-1})^2$$

(see Appendix C of [15]). Utilizing (15) one obtains

$$\begin{aligned}&{\rm s}_\theta^2\,{\rm c}_\theta^2 m_Z^2 Z_H \left(1 - \frac{\delta v}{v}\right)^2 (1 - Z_W Z_{\rm TGV}^{-1})^2 \\ &= \lim_{m\to 0} m^4 \left.\frac{\rm d}{{\rm d}q^2}\right|_{q^2=m^2} \Pi^{\rm T}_{\gamma\gamma}(q^2) = 0,\end{aligned}$$

which yields $Z_{\rm TGV} = Z_W$ or equivalently $\delta Z_{\rm TGV} = \delta Z_W$ and thus

$$\Delta\delta Z_{\rm TGV} = \Delta\delta Z_W. \quad (16)$$

This is the key relation in the following calculation.

4.3 Computation of $\Delta\delta Z_W$

Note first that there is no tadpole contribution to the δZ_W computed by means of (14). This is gratifying in view of the complicated structure of the trilinear Higgs couplings. Defining as usual $\Delta\Pi^{\rm T}_{WW} \equiv [\Pi^{\rm T}_{WW}]_{\rm THDM} - [\Pi^{\rm T}_{WW}]_{\rm SM}$ we can write

$$\Delta\delta Z_W = -\left[\Delta\Pi^{\rm T}_{WW}(m_W^2) + m_W^2 \left.\frac{\rm d}{{\rm d}q^2}\right|_{q^2=m_W^2} \Delta\Pi^{\rm T}_{WW}(q^2)\right].$$

4.3.1 Relevant diagrams

There are only two relevant topologies contributing to $\Delta\delta Z_W$:

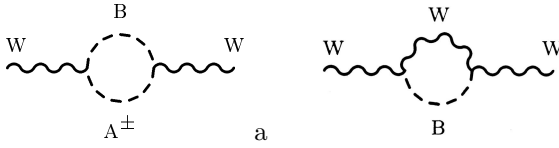

(17)

The two scalar lines in the first graph correspond to the configurations $\{\eta G^\pm\}$ in SM and $\{h^0 G^\pm,\ H^0 G^\pm,\ h^0 H^\pm,\ H^0 H^\pm,\ A^0 H^\pm\}$ in THDM. The internal scalar and vector lines in the second case are $\{\eta W^\pm\}$ in SM and $\{h^0 W^\pm,\ H^0 W^\pm\}$ in THDM. All remaining graphs are common to both models and therefore cancel in the relative quantities.

Using the dimensional regularization with $d = 4 - 2\varepsilon$ the graphs (17a) give

$$\begin{aligned}\Delta\delta Z_W^a = &\left(\sum_{\rm THDM} - \sum_{\rm SM}\right) |g_{WA^\pm B}|^2 \frac{1}{16\pi^2} \quad (18)\\ &\times \left[\frac{1}{3} C_{UV} - 2\int_0^1 {\rm d}x x(1-x) \log \frac{D_x^{A^\pm B}(m_W^2)}{\mu^2}\right],\end{aligned}$$

while the type (17b) yields

$$\Delta\delta Z_W^b = \left(\sum_{\rm THDM} - \sum_{\rm SM}\right) g_{WWB}^2 \frac{1}{16\pi^2} \int_0^1 {\rm d}x \frac{x(1-x)}{D_x^{WB}(m_W^2)}. \quad (19)$$

Here we use the abbreviations

$$\begin{aligned}D_x^{XY}(q^2) &\equiv m_X^2(1-x) + m_Y^2 x - q^2 x(1-x),\\ C_{UV} &\equiv \frac{1}{\varepsilon} - \gamma_E + \log 4\pi.\end{aligned}$$

The explicit expressions for the coupling constants $g_{WA^\pm B}$ and g_{WWB} can be found in Appendix A.2.

4.4 Computation of $\Delta\Pi_i^{VWW}$

Let us first present the list of all diagrams that are not common to both models and therefore do not cancel trivially in $\Delta\Pi_i^{VWW}$. The charged bosons propagating in the loops are denoted by a generic symbol $A^\pm$ and the neutral ones by B and C. All topologies are supplemented by the list of relevant field configurations.

4.4.1 Relevant topologies

The relevant topologies are as follows:

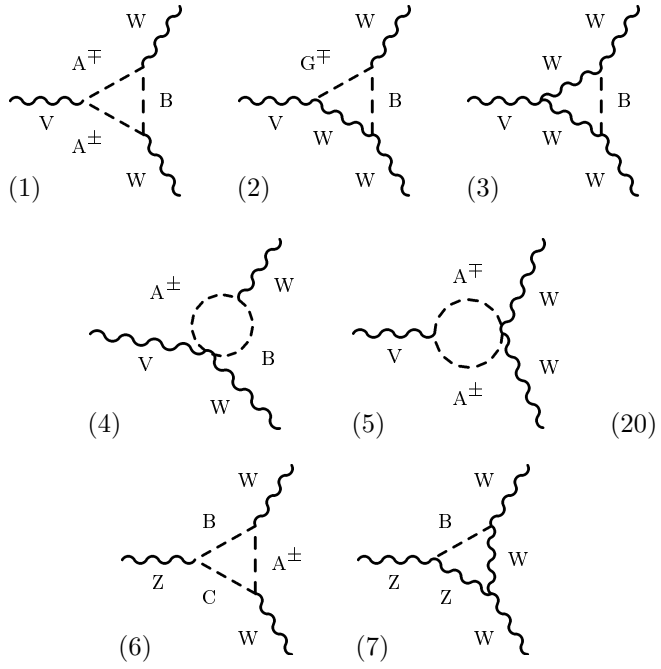

Note that V in (1)–(5) corresponds to γ and Z – these topologies are common to both the $\Delta\Gamma^{\gamma WW}$ and $\Delta\Gamma^{ZWW}$ functions. The graphs (6) and (7) contribute only to $\Delta\Gamma^{ZWW}$.

4.4.2 Relevant field configurations

The configurations of the internal lines denoted by $A^\pm$, B, and C in the Feynman diagrams above can be read off from Table 1.

Note that according to the previous definitions the symbols $\Delta\Gamma^{VWW(i)}$ denote the differences of the contributions coming from the previous graphs with the overall (tree) coupling constants thrown away. Thus, if we denote by $G^{(i)}$ the expressions obtained from these graphs just by using the appropriate Feynman rules, one has

$$-\mathrm{i}c_V\Delta\Gamma^{VWW(j)} \equiv G^{(j)}_{\mathrm{THDM}} - G^{(j)}_{\mathrm{SM}}. \tag{21}$$

The couplings c_V are defined in (3). With all this at hand it is already easy to extract the corresponding $\Delta\Pi_i^{VWW}$ out of $\sum_j \Delta\Gamma^{VWW(j)}$ in accordance with definitions (9) and (13).

4.5 Evaluation of $\Delta\Pi_i^{VWW}$

Let us now summarize the contributions of the graphs (20) to the TGV differences (21). The coupling constants and the integrals appearing in the following expressions can be found in the appendices. The additional numerical factors are usually due to the symmetry properties of the graphs.

Table 1. Field configurations in the triangular graphs (20)

Case	SM and THDM field configurations
(1)	SM: $A^\pm B = G^\pm\eta$
	THDM: $A^\pm B = G^\pm h^0$, $G^\pm H^0$, $H^\pm A^0$, $H^\pm h^0$,$H^\pm H^0$
(2)	SM: $B = \eta$
	THDM: $B = h^0$, H^0
(3)	SM: $B = \eta$
	THDM: $B = h^0$, H^0
(4)	SM: $A^\pm B = G^\pm\eta$
	THDM: $A^\pm B = G^\pm h^0$, $G^\pm H^0$, $H^\pm A^0$, $H^\pm h^0$, $H^\pm H^0$
(5)	SM: $A^\pm$ = nothing
	THDM: $A^\pm = H^\pm$
(6)	SM: $A^\pm BC = G^\pm G^0\eta$
	THDM: $A^\pm BC = G^\pm G^0 h^0$, $G^\pm G^0 H^0$, $H^\pm A^0 h^0$, $H^\pm A^0 H^0$
(7)	SM: $B = \eta$
	THDM: $B = h^0$, H^0

The diagrams (1)–(5) that contribute to both $\Delta\Gamma^{\gamma WW}$ and $\Delta\Gamma^{ZWW}$ yield the expressions

$$-\mathrm{i}c_V\Delta\Gamma^{VWW\,(1)}_{\sigma\mu\nu} = \left(\sum_{\mathrm{THDM}} - \sum_{\mathrm{SM}}\right)\frac{1}{2}g_{VA^+A^-}|g_{WA^\pm B}|^2 \times I^{(1)}_{\sigma\mu\nu}(q_1,-q_2,m_B,m_{A^+},m_{A^-}), \tag{22}$$

$$-\mathrm{i}c_V\Delta\Gamma^{VWW\,(2)}_{\sigma\mu\nu} = \left(\sum_{\mathrm{THDM}} - \sum_{\mathrm{SM}}\right) g_{VWG^\pm}g_{WWB}g^*_{WG^\pm B} \times I^{(2)}_{\sigma\mu\nu}(q_1,-q_2,m_B,m_{G^\pm},m_W), \tag{23}$$

$$-\mathrm{i}c_V\Delta\Gamma^{VWW\,(3)}_{\sigma\mu\nu} = \left(\sum_{\mathrm{THDM}} - \sum_{\mathrm{SM}}\right)\frac{1}{2}g_{VWW}g^2_{WWB} \times I^{(3)}_{\sigma\mu\nu}(q_1,-q_2,m_B,m_W,m_W), \tag{24}$$

$$-\mathrm{i}c_V\Delta\Gamma^{VWW\,(4)}_{\sigma\mu\nu} = \left(\sum_{\mathrm{THDM}} - \sum_{\mathrm{SM}}\right) g_{VWA^\pm B}g^*_{WA^\pm B} \times I^{(4)}_{\sigma\mu\nu}(q_1,-q_2,m_B,m_{A^\pm}), \tag{25}$$

$$-\mathrm{i}c_V\Delta\Gamma^{VWW\,(5)}_{\sigma\mu\nu} = 0.$$

Note that $\Delta\Gamma^{VWW\,(5)}_{\sigma\mu\nu}$ vanishes since it turns out to be proportional to $\int_0^1 \mathrm{d}x(1-2x)\log\left[m^2 - x(1-x)q^2\right]$, which is obviously zero.

Diagrams (6) and (7) provide an extra contribution to $\Delta\Gamma^{ZWW}$:

$$-\mathrm{i}c_Z\Delta\Gamma^{ZWW\,(6)}_{\sigma\mu\nu} = \left(\sum_{\mathrm{THDM}} - \sum_{\mathrm{SM}}\right) g_{ZBC}g_{WA^\pm B}g^*_{WA^\pm C} \times I^{(1)}_{\sigma\mu\nu}(q_1,-q_2,m_{A^\pm},m_C,m_B),$$

$$-\mathrm{i}c_Z \Delta\Gamma^{ZWW\,(7)}_{\sigma\mu\nu} = \left(\sum_{\mathrm{THDM}} - \sum_{\mathrm{SM}}\right) 2 g_{ZZB} g_{WWZ} g_{WWB} \times I^{(5)}_{\sigma\mu\nu}(q_1, -q_2, m_W, m_Z, m_B).$$

The summations are taken with respect to the configurations shown in Table 1.

4.6 Cancellation of UV-divergences

Since we compute the one-loop counterterm $\Delta\delta Z_{\mathrm{TGV}}$ by means of a specific subset of diagrams we should check that the sum of the UV-divergences of $\Delta\Pi_i^{VWW}$ "fit" the divergent part of $\Delta\delta Z_{\mathrm{TGV}}$ to obtain a UV-finite expression for (12).

To proceed, we must first extract the divergent parts of all the $\Delta\Gamma^{VWW\,(j)}_{\sigma\mu\nu}$. Taking into account the prescriptions specified in Appendix B we can see that the only UV-divergent integral we deal with is $I^{(1)}$. In the usual way we can isolate the divergent part of it in the form

$$\mathrm{Div}_{UV}\left[I^{(1)}_{\sigma\mu\nu}(q_1, -q_2, m_j)\right] = -\frac{1}{24\pi^2}\mathrm{C}_{UV} T_{\sigma\mu\nu}.$$

Computing now the total UV-divergences of $\Delta\Gamma^{\gamma WW\,(j)}_{\sigma\mu\nu}$ and $\Delta\Gamma^{ZWW\,(j)}_{\sigma\mu\nu}$ we get

$$\begin{aligned}
&\mathrm{Div}_{UV}\left[\sum_j \Delta\Gamma^{\gamma WW\,(j)}_{\sigma\mu\nu}\right] = \mathrm{Div}_{UV}\left[\Delta\Gamma^{\gamma WW\,(1)}_{\sigma\mu\nu}\right] \\
&= -\frac{\mathrm{i}}{e}\left(\sum_{\mathrm{THDM}} - \sum_{\mathrm{SM}}\right) g_{\gamma A^+A^-} |g_{WA^\pm B}|^2 \frac{1}{48\pi^2}\mathrm{C}UVT_{\sigma\mu\nu} \\
&= -\frac{1}{96\pi^2}\frac{e^2}{\sin^2\theta}\mathrm{C}UVT_{\sigma\mu\nu} \qquad (26)
\end{aligned}$$

In the case of $\Delta\Gamma^{ZWW}$ we have two UV-divergent topologies, namely

$$\begin{aligned}
&\mathrm{Div}_{UV}\left[\sum_j \Delta\Gamma^{ZWW\,(j)}_{\sigma\mu\nu}\right] \\
&= \mathrm{Div}_{UV}\left[\Delta\Gamma^{ZWW\,(1)}_{\sigma\mu\nu}\right] + \mathrm{Div}_{UV}\left[\Delta\Gamma^{ZWW\,(6)}_{\sigma\mu\nu}\right] \\
&= -\frac{\mathrm{i}}{e\cot\theta}\left(\sum_{\mathrm{THDM}} - \sum_{\mathrm{SM}}\right) \\
&\quad \times \left(g_{\gamma A^+A^-}|g_{WA^\pm B}|^2 + g_{ZBC} g_{WA^\pm B} g^\dagger_{WA^\pm C}\right) \\
&= \frac{1}{48\pi^2}\mathrm{C}UVT_{\sigma\mu\nu} = -\frac{1}{96\pi^2}\frac{e^2}{\sin^2\theta}\mathrm{C}UVT_{\sigma\mu\nu}.
\end{aligned}$$

From this we can conclude that

$$\mathrm{Div}_{UV}\left[\Delta\Pi^{ZWW}_{1,2,3}\right] = \mathrm{Div}_{UV}\left[\Delta\Pi^{\gamma WW}_{1,2,3}\right] = -\frac{1}{96\pi^2}\frac{e^2}{\sin^2\theta}\mathrm{C}UV,$$

$$\mathrm{Div}_{UV}\left[\Delta\Pi^{ZWW}_{4,5,6,7}\right] = \mathrm{Div}_{UV}\left[\Delta\Pi^{\gamma WW}_{4,5,6,7}\right] = 0. \quad (27)$$

Next, the divergent part of $\Delta\delta Z_{\mathrm{TGV}}$ can be easily derived from (18):

$$\begin{aligned}
\mathrm{Div}_{UV}\left[\Delta\delta Z_W\right] &= \frac{1}{3}\left(\sum_{\mathrm{THDM}} - \sum_{\mathrm{SM}}\right) |g_{WA^\pm B}|^2 \frac{1}{16\pi^2} C_{UV} \\
&= \frac{1}{96\pi^2}\frac{e^2}{\sin^2\theta_{\mathrm{W}}} C_{UV}. \qquad (28)
\end{aligned}$$

Comparing (27) with (28) we can conclude that the UV-divergences in (12) cancel exactly as expected.

5 Computation of $\Delta\Gamma^{\gamma WW}$ and $\Delta\Gamma^{ZWW}$

In view of the large number of relevant Feynman graphs it is not feasible to display all the general results in detail. This is mainly because of the Passarino–Veltman (PV) reduction which is traditionally used to "scalarize" the tensorial structure of the resulting integrals [17, 18].

Therefore we will only describe briefly some salient points, in particular the origin of the possible non-decoupling effects of heavy virtual Higgses.

5.1 Finite part of $\Delta\delta Z_{\mathrm{TGV}}$

The mass dependence of the counterterms can be read off from (18) and (19). Assuming the masses of the THDM Higgs bosons to be well above m_W we can estimate the value of $\Delta\delta Z^b_W$ to be less than about 10^{-4} (and falling with $m_H, m_h \to \infty$) i.e. small compared to the expected order of magnitude of non-decoupling effects (10^{-2}–10^{-3}).

The situation in the case of $\Delta\delta Z^a_W$ is more subtle because of the presence of the μ scale in the logarithm in (18). However, due to the above-mentioned cancellation of divergences (4.6) the overall one-loop renormalized Green functions are μ-independent and we can either choose some particular value of μ or combine that term with the corresponding μ-dependent factor from the $\Delta\Pi^i$ to obtain μ-independent quantities and discuss both these pieces together.

Note that the behavior of the counterterms is scheme-dependent. For example in MS or $\overline{\mathrm{MS}}$ the finite parts of $\Delta\delta Z^{a,b}_W$ are constant while in the on-shell scheme they typically grow logarithmically with masses of the Higgs particles in the loops. However, since they are strongly suppressed with respect to the finite parts of the $\Delta\Pi_i$, this scheme-dependence is practically negligible.

5.2 Finite parts of the $\Delta\Pi_i$

Concerning the structure of integrals contributing to the $\Delta\Pi$ (Appendix B), one finds that the possible non-decoupling effects in the large heavy Higgs mass regime (keeping

m_η and m_{h^0} at the weak scale) can descend only from the divergent factors $C_{\alpha\beta\gamma}$, $C_{\alpha\beta}$, B_α and B_0; all the others (UV-finite) tend to zero. Note that in some situations the straightforward $m_{\rm heavy} \to \infty$ limit is not meaningful because in such a case the Higgs self-couplings may blow up, and the perturbative approach used here is then no longer valid; see below.

Next, the mass dependence of the B-terms seems to be much weaker compared to the highly polynomial factors in $C_{\alpha\beta\gamma}$. On the other hand, the apparent powerlike behavior of the PV coefficients in the expansions of the $C_{\alpha\beta\gamma}$ is often compensated by the powers of heavy Higgs masses in the denominators of the PV scalar integrals C_0, and thus there is no reason to suppress the B-terms relative to the C-terms.

As an illustration, consider the combination $C_{\alpha\beta\gamma}(p_1, p_2, m_0, m_1, m_2) + \text{sym.}$ in $I^{(1)}_{\alpha\beta\gamma}$ entering the $\Delta\Pi^{VWW}_{1,2,3}$ *on-shell*, i.e. taking $p_1^2 = p_2^2 = m_W^2$, $(p_1+p_2)^2 = s$. First note that this quantity is dimensionless. Bearing in mind how the PV reduction works we can expect coefficients of three basic types (here $\tilde{B}_0$ denotes the finite part of B_0, k is integer, and $n = 0, 1, 2, \ldots$):

$$\begin{aligned} &(a) \qquad M_i^{6-n} s^k m_W^{-2k+n} C_0(p^2, \ldots, M_i^2, \ldots), \\ &(b) \qquad M_i^{4-n} s^k m_W^{-2k+n} \tilde{B}_0(p^2, M_i^2, \ldots), \\ &(c) \qquad M_i^{2-n} s^k m_W^{-2k+n-2}. \end{aligned} \tag{29}$$

A typical contribution to $\Delta\Pi^{VWW}_{1,2,3}$ then looks like

$$\Delta\Pi^{VWW}_{1,2,3} \sim \frac{f}{16\pi^2} |g_{WA^\pm B}|^2 \times X + \ldots,$$

with X being an expression from the set (29). Here f is an $O(1)$ numerical factor; $g_{WA^\pm B}$ are the couplings. Though it seems that the leading terms are of the order M_i^6, such a growth is in fact reduced by factors involving negative powers of masses, coming from denominators of the C_0 functions in the heavy Higgs mass regime. The suppression is even stronger once the parameters obey the decoupling limit behavior; see below. Therefore one has to be very careful in semiquantitative arguments based on (29).

Unfortunately, due to the enormous complexity of the results it is almost hopeless to try to get simple general analytic expressions for the leading terms in the $\Delta\Pi_i^{VWW}$ even in the heavy Higgs mass regime. Next, it is worth *focusing in particular to the cases when one cannot expect the decoupling of the additional Higgs bosons in the Appelquist–Carazzone manner.*

For such setups we have performed at least a simple numerical analysis with the following results[1].
(1) The leading terms in the $|\Delta\Pi_i^{VWW}|$ typically contain logarithms and inverse powers of the heavy Higgs masses, i.e.

$$|\Delta\Pi_i^{VWW}| \sim \frac{f}{16\pi^2} |g_1 g_2^*| \left[k_1 \log \frac{m_{\rm Higgs}}{m_W} + k_2\, O(m_W m_{\rm Higgs}^{-1}) \right] + \ldots$$

This means that the larger the Higgs masses are, the smoother the $\Delta\Pi_i^{VWW}$ behave and their behavior tends to be purely logarithmic (of course, with $k_1 \to 0$ in the decoupling regime).
(2) The overall magnitudes of $|\Delta\Pi_i^{VWW}|$ usually turn out to be around 10^{-3} (at $m_{\rm Higgs} \sim m_W$), so the possible large non-decoupling effects in physical amplitudes seem to be quite unlikely, barring some special enhancements coming from kinematics and/or geometrical factors [12].

Let us illustrate these features in the case of $|\Delta\Pi_1^{VWW}|$ and $|\Delta\Pi_2^{VWW}|$ within one of the concrete realizations of the Higgs sector of the model. Although the Higgs self-couplings do not enter explicitly our analysis, their values determine the shape of the Higgs spectrum of the model which must be chosen in a way compatible with these constraints. In other words, shifting the heavy Higgs masses and holding at the same time some of the features of the Higgs potential unchanged causes a shift in the mixing angles α and β which propagates via $\sin(\alpha-\beta)$ and $\cos(\alpha-\beta)$ to the vector-boson–Higgs couplings.

For simplicity, we take[2]

$$\lambda_6 = \lambda_7 = 0, \qquad m_{12} = 0, \tag{30}$$

and especially

$$\lambda_1 = \lambda_2 \equiv \lambda, \qquad \lambda_3 = 1 \quad \text{and} \quad \beta = \pi/2.$$

The remaining parameters λ, λ_4, λ_5 α, m_1 and m_2 are then driven by the choice of m_h, m_H, m_A, $m_{H^\pm}$ so that the resulting Higgs potential produces the right mass pattern.

For example, let us display in Figs. 1 and 2 the behavior of the $|\Delta\Pi_1^{\gamma WW}|$ and $|\Delta\Pi_1^{\gamma WW}|$ in this model as functions of the m_{A^0} parameter. The other parameters are fixed as follows: $m_\eta = 105\,\text{GeV}$, $m_{h^0} = 125\,\text{GeV}$, $m_{H^0} = 145\,\text{GeV}$, $m_{H^\pm} = 180\,\text{GeV}$, $\sqrt{s} = 250\,\text{GeV}$. As was stated above, these quantities grow logarithmically (in the non-decoupling setup (30)) with the mass of the relatively heavy m_A^0 boson in the model.

[1] We have also checked the proper decoupling behavior of the form factors in the cases that the heavy Higgs sector has been adjusted towards the decoupling regime; this provides a simple consistency check of the results.

[2] N.B. It is well known that the choice (30) provides a setup in which the heavy Higgs mass limit does not exist at all [5], i.e. we cannot push the Higgs masses too far beyond the weak scale. This is caused by the fact that in this setup all the THDM Higgs masses must be of the same order:

$$m_h^2 + m_H^2 = \lambda v^2, \qquad m_A^2 = -\,\mathrm{Re}\,\lambda_5 v^2,$$

$$m_{H^\pm}^2 = -\frac{1}{2}(\lambda_4 + \mathrm{Re}\,\lambda_5) v^2,$$

Then the only way to get large masses of H, A and $H^\pm$ consists in having λ, $|\lambda_4|$ and $\mathrm{Re}\,\lambda_5$ well above 1. In other words, it is exactly one of the physically interesting situations in which one can expect non-decoupling behavior of the heavy part of the THDM Higgs spectrum and some (in principle) measurable deviations from the SM predictions; for further details see for example [12].
The main advantage of the choice is the simplicity of the relation for $\cos^2(\alpha-\beta)$ which is the basic ingredient of any quantitative analysis.

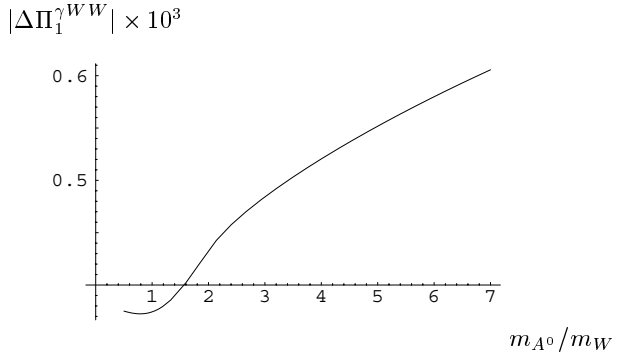

Fig. 1. Behavior of the $|\Delta\Pi_1^{\gamma WW}|$ as function of the m_{A^0} parameter

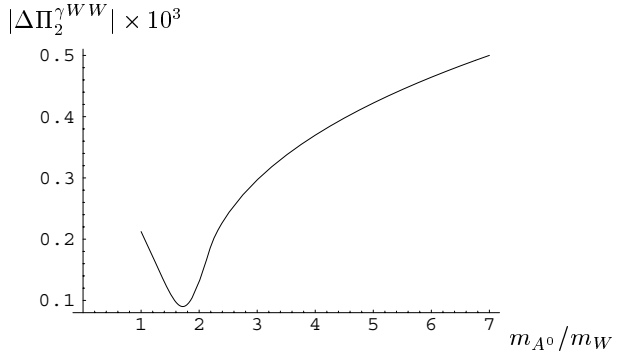

Fig. 2. Behavior of $|\Delta\Pi_1^{\gamma WW}|$ as function of the m_{A^0} parameter

6 Conclusion

We have computed the additional contributions to the one-loop THDM triple gauge vertices which are not present within the SM framework. The model is taken to be very general [14] with no need of any additional constraints to its structure.

We have adopted the on-shell renormalization scheme, using the dimensional regularization of UV-divergences. The finite parts of the on-shell counterterms are computed with the help of the W-boson propagator renormalization constants. Cancellation of UV-divergences is checked explicitly in both the γWW and ZWW case.

The THDM heavy Higgs boson contributions to the triple gauge vertices can in some situations lead to possible non-decoupling effects in physical amplitudes. Therefore, these results can be employed (at least in principle) for an indirect exploration of the structure of the electroweak Higgs sector at future collider facilities.

Acknowledgements. This work was supported by "Centre for Particle Physics", project No. LN00A006 of the Ministry of Education of the Czech Republic.

A THDM interactions of vector bosons

A.1 Relevant part of THDM lagrangian

The lagrangian (2) can be decomposed into three parts corresponding to VHH, VVH and VVHH vertices respectively:

$$\mathcal{L}^{\rm kin}_{\rm Higgs} == \mathcal{L}_{VVH} + \mathcal{L}_{VHH} + \mathcal{L}_{VVHH} + \text{other terms.}$$

Here

$$\begin{aligned}
&\mathcal{L}_{VVH} \\
&= em_Z \cot\theta_{\rm W} W^{+\mu} W^-_\mu \left[H^0\cos(\alpha-\beta) - h^0\sin(\alpha-\beta)\right] \\
&+ \frac{em_Z}{\sin 2\theta_{\rm W}} Z^\mu Z_\mu \left[H^0\cos(\alpha-\beta) - h^0\sin(\alpha-\beta)\right] \\
&+ em_Z\left(\cos\theta_{\rm W} A^\mu - \sin\theta_{\rm W} Z^\mu\right)\left(W^+_\mu G^- + W^-_\mu G^+\right)
\end{aligned}$$

and

$$\begin{aligned}
&\mathcal{L}_{VHH} = {\rm i}eA^\mu H^+ \partial^\leftrightarrow_\mu H^- + {\rm i}eA^\mu G^+ \partial^\leftrightarrow_\mu G^- \\
&+ {\rm i}e\cot 2\theta_{\rm W} Z^\mu H^+ \partial^\leftrightarrow_\mu H^- + {\rm i}e\cot 2\theta_{\rm W} Z^\mu G^+ \partial^\leftrightarrow_\mu G^- \\
&+ \frac{e}{\sin 2\theta_{\rm W}} \\
&\times \left\{ Z^\mu \left[\cos(\alpha-\beta) A^0 \partial^\leftrightarrow_\mu h^0 - \sin(\alpha-\beta) G^0 \partial^\leftrightarrow_\mu h^0\right]\right. \\
&+ Z^\mu \left[\sin(\alpha-\beta) A^0 \partial^\leftrightarrow_\mu H^0 + \cos(\alpha-\beta) G^0 \partial^\leftrightarrow_\mu H^0\right] \\
&- \cos(\alpha-\beta)\left(W^{-\mu} h^0 \partial^\leftrightarrow_\mu H^+ + W^{+\mu} H^- \partial^\leftrightarrow_\mu h^0\right) \\
&+ \sin(\alpha-\beta)\left(W^{-\mu} h^0 \partial^\leftrightarrow_\mu G^+ + W^{+\mu} G^- \partial^\leftrightarrow_\mu h^0\right) \\
&- \sin(\alpha-\beta)\left(W^{-\mu} H^0 \partial^\leftrightarrow_\mu H^+ + W^{+\mu} H^- \partial^\leftrightarrow_\mu H^0\right) \\
&- \cos(\alpha-\beta)\left(W^{-\mu} H^0 \partial^\leftrightarrow_\mu G^+ + W^{+\mu} G^- \partial^\leftrightarrow_\mu H^0\right) \\
&- \left(W^{-\mu} A^0 \partial^\leftrightarrow_\mu H^+ - W^{+\mu} H^- \partial^\leftrightarrow_\mu A^0\right) \\
&\qquad \left.- \left(W^{-\mu} G^0 \partial^\leftrightarrow_\mu G^+ - W^{+\mu} G^- \partial^\leftrightarrow_\mu G^0\right)\right\},
\end{aligned}$$

while

$$\begin{aligned}
&\mathcal{L}_{VVHH} = \frac{e^2}{2\sin^2\theta_{\rm W}} W^{+\mu} W^-_\mu \left[H^+H^- + G^+G^-\right] \\
&+ \frac{e^2}{4\sin^2\theta_{\rm W}} W^{+\mu} W^-_\mu \left[(h^0)^2 + (H^0)^2 + (A^0)^2 + (G^0)^2\right] \\
&+ \frac{e^2}{2\sin\theta_{\rm W}} A^\mu \left[H^0\cos(\alpha-\beta) - h^0\sin(\alpha-\beta)\right] \\
&\qquad \times \left(W^+_\mu G^- + W^-_\mu G^+\right) \\
&+ \frac{e^2}{2\sin\theta_{\rm W}} A^\mu \left[H^0\sin(\alpha-\beta) + h^0\cos(\alpha-\beta)\right] \\
&\qquad \times \left(W^+_\mu H^- + W^-_\mu H^+\right) - \\
&- \frac{e^2}{2\cos\theta_{\rm W}} Z^\mu \left[H^0\cos(\alpha-\beta) - h^0\sin(\alpha-\beta)\right] \\
&\qquad \times \left(W^+_\mu G^- + W^-_\mu G^+\right) -
\end{aligned}$$

$$
\begin{aligned}
&- \frac{e^2}{2\cos\theta_{\mathrm{W}}} Z^\mu \left[H^0 \sin(\alpha-\beta) + h^0 \cos(\alpha-\beta)\right] \\
&\qquad \times \left(W^+_\mu H^- + W^-_\mu H^+\right) \\
&+ \frac{\mathrm{i}e^2}{\sin 2\theta_{\mathrm{W}}} G^0 \left(\cos\theta_{\mathrm{W}} A^\mu - \sin\theta_{\mathrm{W}} Z^\mu\right) \\
&\qquad \times \left(W^+_\mu G^- - W^-_\mu G^+\right) \\
&+ \frac{\mathrm{i}e^2}{\sin 2\theta_{\mathrm{W}}} A^0 \left(\cos\theta_{\mathrm{W}} A^\mu - \sin\theta_{\mathrm{W}} Z^\mu\right) \\
&\qquad \times \left(W^+_\mu H^- - W^-_\mu H^+\right).
\end{aligned}
$$

A.2 Coupling constants

As before, the charged (pseudo-) scalars are denoted by the generic symbols $A^\pm$, while the neutral ones are written B and C. We compile the coupling constants in Tables 2–5.

Table 2. VVHH type

$A^\pm B$	$g_{\gamma W A^\pm B}$	$g_{ZW A^\pm B}$
$G^\pm\eta$	$\frac{1}{2}\mathrm{i}e^2\,\mathrm{cs}_\theta$	$-\frac{1}{2}\mathrm{i}e^2\,\mathrm{sc}_\theta$
$G^\pm h^0$	$-\frac{1}{2}\mathrm{i}e^2\,\mathrm{cs}_\theta\,\mathrm{s}_{\alpha-\beta}$	$\frac{1}{2}\mathrm{i}e^2\,\mathrm{sc}_\theta\,\mathrm{s}_{\alpha-\beta}$
$G^\pm H^0$	$\frac{1}{2}\mathrm{i}e^2\,\mathrm{cs}_\theta\,\mathrm{c}_{\alpha-\beta}$	$-\frac{1}{2}\mathrm{i}e^2\,\mathrm{sc}_\theta\,\mathrm{c}_{\alpha-\beta}$
$H^\pm h^0$	$\frac{1}{2}\mathrm{i}e^2\,\mathrm{cs}_\theta\,\mathrm{c}_{\alpha-\beta}$	$-\frac{1}{2}\mathrm{i}e^2\,\mathrm{sc}_\theta\,\mathrm{c}_{\alpha-\beta}$
$H^\pm H^0$	$\frac{1}{2}\mathrm{i}e^2\,\mathrm{cs}_\theta\,\mathrm{s}_{\alpha-\beta}$	$-\frac{1}{2}\mathrm{i}e^2\,\mathrm{sc}_\theta\,\mathrm{s}_{\alpha-\beta}$
$G^\pm G^0$	$-\frac{1}{2}e^2\,\mathrm{cs}_\theta$	$\frac{1}{2}e^2\,\mathrm{sc}_\theta$
$H^\pm A^0$	$-\frac{1}{2}e^2\,\mathrm{cs}_\theta$	$\frac{1}{2}e^2\,\mathrm{sc}_\theta$

Table 3. VHH type

BC	g_{ZBC}
$G^0\eta$	$-e\,\mathrm{cs}_{2\theta}$
$G^0 h^0$	$e\,\mathrm{cs}_{2\theta}\,\mathrm{s}_{\alpha-\beta}$
$G^0 H^0$	$-e\,\mathrm{cs}_{2\theta}\,\mathrm{c}_{\alpha-\beta}$
$A^0 h^0$	$-e\,\mathrm{cs}_{2\theta}\,\mathrm{c}_{\alpha-\beta}$
$A^0 H^0$	$-e\,\mathrm{cs}_{2\theta}\,\mathrm{s}_{\alpha-\beta}$

$A^\pm B$	$g_{W A^\pm B}$
$G^\pm\eta$	$\frac{1}{2}\mathrm{i}e\,\mathrm{cs}_\theta$
$G^\pm h^0$	$-\frac{1}{2}\mathrm{i}e\,\mathrm{cs}_\theta\,\mathrm{s}_{\alpha-\beta}$
$G^\pm H^0$	$\frac{1}{2}\mathrm{i}e\,\mathrm{cs}_\theta\,\mathrm{c}_{\alpha-\beta}$
$H^\pm h^0$	$\frac{1}{2}\mathrm{i}e\,\mathrm{cs}_\theta\,\mathrm{c}_{\alpha-\beta}$
$H^\pm H^0$	$\frac{1}{2}\mathrm{i}e\,\mathrm{cs}_\theta\,\mathrm{s}_{\alpha-\beta}$
$G^\pm G^0$	$-\frac{1}{2}e\,\mathrm{cs}_\theta$
$H^\pm A^0$	$-\frac{1}{2}e\,\mathrm{cs}_\theta$

A^+A^-	$g_{\gamma A^+A^-}$	$g_{ZA^+A^-}$
G^+G^-	$-\mathrm{i}e$	$-\mathrm{i}e\,\mathrm{ct}_{2\theta}$
H^+H^-	$-\mathrm{i}e$	$-\mathrm{i}e\,\mathrm{ct}_{2\theta}$

Table 4. VVH type

B	g_{ZZB}	g_{WWB}
η	$\mathrm{i}em_Z\,\mathrm{cs}_{2\theta}$	$\mathrm{i}em_Z\,\mathrm{ct}_\theta$
h^0	$-\mathrm{i}em_Z\,\mathrm{cs}_{2\theta}\,\mathrm{s}_{\alpha-\beta}$	$-\mathrm{i}em_Z\,\mathrm{ct}_\theta\,\mathrm{s}_{\alpha-\beta}$
H^0	$\mathrm{i}em_Z\,\mathrm{cs}_{2\theta}\,\mathrm{c}_{\alpha-\beta}$	$\mathrm{i}em_Z\,\mathrm{ct}_\theta\,\mathrm{c}_{\alpha-\beta}$

$g_{\gamma WG^\pm}$	$= \mathrm{i}em_Z\,\mathrm{c}_\theta$
$g_{ZWG^\pm}$	$= -\mathrm{i}em_Z\,\mathrm{s}_\theta$

Table 5. VVV type

$g_{\gamma WW}$	$= -\mathrm{i}e$
g_{ZWW}	$= -\mathrm{i}e\,\mathrm{ct}_\theta$

B Useful integrals

At this place we display all necessary loop integrals in terms of the Passarino–Veltman functions [16–18] listed below:

$$
\begin{aligned}
&I^{(1)}_{\alpha\beta\gamma}(p_1,p_2,m_0,m_1,m_2) \equiv \begin{pmatrix}\beta\leftrightarrow\gamma\\ p_1\leftrightarrow p_2\end{pmatrix} \\
&+\mu^{2\varepsilon}\mathrm{i}^3\int\frac{\mathrm{d}^dk}{(2\pi)^d} \\
&\times\frac{-(2k+p_1+p_2)_\alpha(2k+p_1)_\beta(2k+p_2)_\gamma}{(k^2-m_0^2)\left[(k+p_1)^2-m_1^2\right]\left[(k+p_2)^2-m_2^2\right]} = \\
&-\frac{1}{16\pi^2}\left[8C_{\alpha\beta\gamma}+4(p_1+p_2)_\alpha C_{\beta\gamma}+4p_{1\beta}C_{\alpha\gamma}+4p_{2\gamma}C_{\alpha\beta}\right. \\
&+2(p_1+p_2)_\alpha p_{1\beta}C_\gamma+2(p_1+p_2)_\alpha p_{2\gamma}C_\beta+2p_{1\beta}p_{2\gamma}C_\alpha \\
&\left.+\,(p_1+p_2)_\alpha p_{1\beta}p_{2\gamma}C_0\right](p_1,p_2,m_0,m_1,m_2) \\
&+(p_1\leftrightarrow p_2,\beta\leftrightarrow\gamma), \\
&I^{(2)}_{\alpha\beta\gamma}(p_1,p_2,m_0,m_1,m_2) \equiv \begin{pmatrix}\beta\leftrightarrow\gamma\\ p_1\leftrightarrow p_2\end{pmatrix} \\
&+\mu^{2\varepsilon}\mathrm{i}\int\frac{\mathrm{d}^dk}{(2\pi)^d} \\
&\times\frac{g_{\alpha\gamma}(2k+p_1)_\beta}{(k^2-m_0^2)\left[(k+p_1)^2-m_1^2\right]\left[(k+p_2)^2-m_2^2\right]} = \\
&-\frac{1}{16\pi^2}g_{\alpha\gamma}\left[2C_\beta+p_{1\beta}C_0\right](p_1,p_2,m_0,m_1,m_2) \\
&+(p_1\leftrightarrow p_2,\beta\leftrightarrow\gamma), \qquad (31) \\
&I^{(3)}_{\alpha\beta\gamma}(p_1,p_2,m_0,m_1,m_2) \equiv (p_1\leftrightarrow p_2,\beta\leftrightarrow\gamma) \\
&+\mu^{2\varepsilon}\mathrm{i}^3\int\frac{\mathrm{d}^dk}{(2\pi)^d} \\
&\times\frac{g_{\beta\gamma}(2k+p_1+p_2)_\alpha-g_{\alpha\gamma}(2p_2-p_1+k)_\beta-g_{\alpha\beta}(2p_1-p_2+k)_\gamma}{(k^2-m_0^2)\left[(k+p_1)^2-m_1^2\right]\left[(k+p_2)^2-m_2^2\right]} \\
&=\frac{1}{16\pi^2}\left\{2g_{\beta\gamma}C_\alpha-g_{\alpha\gamma}C_\beta-g_{\alpha\beta}C_\gamma+\left[g_{\beta\gamma}(p_1+p_2)_\alpha\right.\right. \\
&\left.\left.-\,g_{\alpha\gamma}(2p_2-p_1)_\beta-g_{\alpha\beta}(2p_1-p_2)_\gamma\right]C_0\right\}(p_1,p_2,m_0,m_1,m_2) \\
&+(p_1\leftrightarrow p_2,\beta\leftrightarrow\gamma),
\end{aligned}
$$

$$
\begin{aligned}
&I^{(4)}_{\alpha\beta\gamma}(p_1,p_2,m_0,m_1)\\
&\equiv \mu^{2\varepsilon}\mathrm{i}^2\int\frac{\mathrm{d}^dk}{(2\pi)^d}\\
&\times\frac{g_{\alpha\gamma}(2k+p_1)_\beta}{(k^2-m_0^2)\left[(k+p_1)^2-m_1^2\right]}+\begin{pmatrix}\beta\leftrightarrow\gamma\\ p_1\leftrightarrow p_2\end{pmatrix}\\
&=-\frac{\mathrm{i}}{16\pi^2}g_{\alpha\gamma}\left[2B_\beta+p_{1\beta}B_0\right](p_1,m_0,m_1)\\
&+(p_1\leftrightarrow p_2,\beta\leftrightarrow\gamma),\\
&I^{(5)}_{\alpha\beta\gamma}(p_1,p_2,m_0,m_1,m_2)\equiv\begin{pmatrix}\beta\leftrightarrow\gamma\\ p_1\leftrightarrow p_2\end{pmatrix}\\
&+\mu^{2\varepsilon}\mathrm{i}^3\int\frac{\mathrm{d}^dk}{(2\pi)^d}\\
&\times\frac{g_{\beta\gamma}(p_1-k)_\alpha+g_{\alpha\gamma}(2k+p_1)_\beta-g_{\alpha\beta}(2p_1+k)_\gamma}{(k^2-m_0^2)\left[(k+p_1)^2-m_1^2\right]\left[(k+p_2)^2-m_2^2\right]}\\
&=\frac{1}{16\pi^2}\left\{-g_{\beta\gamma}C_\alpha+2g_{\alpha\gamma}C_\beta-g_{\alpha\beta}C_\gamma\right.\\
&+\left.\left[g_{\beta\gamma}p_{1\alpha}+g_{\alpha\gamma}p_{1\beta}-g_{\alpha\beta}2p_{1\gamma}\right]C_0\right\}(p_1,p_2,m_0,m_1,m_2)\\
&+(p_1\leftrightarrow p_2,\beta\leftrightarrow\gamma).
\end{aligned}
$$

The Passarino–Veltman functions are defined as

$$
\begin{aligned}
&\frac{\mathrm{i}}{16\pi^2}B_0,B_\alpha,B_{\alpha\beta}(p,m_0,m_1)\\
&\equiv\mu^{2\varepsilon}\int\frac{\mathrm{d}^dk}{(2\pi)^d}\frac{1,k_\alpha,k_{\alpha\beta}}{(k^2-m_0^2)\left[(k+p)^2-m_1^2\right]}\\
&\times\frac{\mathrm{i}}{16\pi^2}C_0,C_\alpha,C_{\alpha\beta},C_{\alpha\beta\gamma}(p_1,p_2,m_0,m_1,m_2)\\
&\equiv\mu^{2\varepsilon}\int\frac{\mathrm{d}^dk}{(2\pi)^d}\\
&\times\frac{1,k_\alpha,k_\alpha k_\beta,k_\alpha k_\beta k_\gamma}{(k^2-m_0^2)\left[(k+p_1)^2-m_1^2\right]\left[(k+p_2)^2-m_2^2\right]}
\end{aligned}
$$

(calculations are performed in dimension $d=4-2\varepsilon$, propagators are displayed without the "$+\mathrm{i}\eta$" factors).

References

1. T.D. Lee, Phys. Rev. D **8**, 1226 (1973)
2. M. Sher, Phys. Rept. **179**, 273 (1989)
3. E.O. Iltan, Phys. Rev. D **65**, 036003 (2002) [hep-ph/0108230]
4. M. Krawczyk, Acta Phys. Polon. B **33**, 2621 (2002) [hep-ph/0208076]
5. J.F. Gunion, H.E. Haber, Phys. Rev. D **67**, 075019 (2003) [hep-ph/0207010]
6. S. Kanemura, S. Kiyoura, Y. Okada, E. Senaha, C.P. Yuan, Phys. Lett. B **558**, 157 (2003) [hep-ph/0211308]
7. R.A.D. Sanchez, Ph.D. thesis [hep-ph/0212237]
8. T. Appelquist, J. Carazzone, Phys. Rev. D **11**, 2856 (1975)
9. A. Dobado, M.J. Herrero, S. Penaranda, Eur. Phys. J. C **17**, 487 (2000) [hep-ph/0002134]
10. S. Kanemura, H.A. Tohyama, Phys. Rev. D **57**, 2949 (1998) [hep-ph/9707454]
11. J.M. Cornwall, D.N. Levin, G. Tiktopoulos, Phys. Rev. D **10**, 1145 (1974) [Erratum D **11**, 972 (1975)]
12. M. Malinský, J. Hořejší, $e^+e^-\to W^+W^-$ in THDM, in preparation
13. M. Malinský, Acta Phys. Slov. **52**, 259 (2002) [hep-ph/0207066]
14. J.F. Gunion, H.E. Haber, G.L. Kane, S. Dawson, The Higgs hunter's guide (Perseus Publishing, Cambridge, Massachusetts 2000)
15. S. Pokorski, Gauge field theories, 2nd edition (Cambridge University Press, Cambridge 2000)
16. M. Bohm, A. Denner, T. Sack, W. Beenakker, F.A. Berends, H. Kuijf, Nucl. Phys. B **304**, 463 (1988)
17. G. Passarino, M.J. Veltman, Nucl. Phys. B **160**, 151 (1979)
18. D.Y. Bardin, G. Passarino, The standard model in the making: Precision study of the electroweak interactions (Clarendon, Oxford, UK 1999)